Predicting glare from daylight through microstructures solar control systems using matrix-based simulation methods in Radiance
Building Simulation 2022 Conference, Copenhagen

Emil P. O. Kjeldsen[1,2], Helle Foldbjerg Rasmussen[1], Mandana, S. Khanie[2]
[1]MicroShade A/S, Glostrup, Denmark
[2]Technical University of Denmark, Kgs. Lyngby, Denmark

Abstract

In this study the five-phase method and a parallelized invocation of `evalglare` has been used, to evaluate the performance of a microstructure and a Low-E window w/wo external blind, in terms of glare. The first part of the results investigates how Bidirectional-Scattering-Distribution-Functions, BSDF, and aBSDF (Aperture BSDF) properties bias the predicted glare through a microstructure, linking BSDF rank to saturation glare and resolution to contrast glare. The investigation found a combination of correct rank, low resolution and peak extraction (aBSDF) to be the best trade-off between speed and accuracy. The later comparison found none of the investigated systems to be sufficient glare protection. The microstructure was found to outperform the external blinds, using the current shading schedule (9% peak difference in occupied hours exceeding a DGP of 0.45).

Introduction

Predicting glare has always been one of the more challenging aspects of daylight simulations, as it combines the human sensation of visual discomfort with measurements, ray-tracing and image handling algorithms, like `evalglare`. One of the primary ray-tracing engines used for conducting scientific daylight simulations is radiance. Though radiance is mainly utilized through third-party software on Windows OS as the engine running under the hood, much time can be saved if the simulations are conducted directly in a Linux version of Radiance with the proper hardware, as this version allows for parallelized ray-tracing and full user control. By using *Windows Subsystem Linux*, WSL, it has in recent years become possible to do this on a windows computer without a hard-drive partition. The workflow presented in this paper provides an easy-to-use simulation procedure for conducting annual image-based simulations using the five-phase method and subsequent glare calculations using `evalglare`. The workflow is written in the Linux native command language Bash (Bourne Again Shell). The workflow is used to investigate the level of glare yielded by different resolutions and ranks of tensor tree BSDFs, of a microstructure fenestration system, on an annual basis.

Methodology

The simulation work conducted in this study revolves around a simulation workflow in BASH, prepared to be easy to use. The workflow consist of two parts, one for conducting the five-phase simulation (McNeil (2013); Geisler-Moroder et al. (2017); Subramaniam (2017)), and one for conducting the glare analysis with `evalglare` (Wienold and Christoffersen (2006)). The workflow requires the user to prepare some inputs which are assigned in the main-script. From the main-script, the specific simulation steps can also be selected and deselected. The inputs that should be prepared is:

- Room geometry
- Window geometry
- View specification (For glare purposes use 180° field-of-view and -vta view type)
- Materials of the room surfaces
- A full Klems resolution and a tensor tree BSDF (use e.g. `genBSDF` (McNeil (2015)) for this step)
- A weather file of the location of interest (EPW or WEA format).

Additional inputs are also to be given in the main-script, including simulation ID, number of CPUs and image resolution. It should be kept in mind, that the recommended image resolution for `evalglare` is 1000x1000 pixels (`evalglare` manual page). When the inputs are prepared and assigned in the main-script, the next step is to run the five-phase simulation. Hence:

- Conduct an initial three-phase simulation.
- Conduct a second three-phase simulation only considering the direct sunlight.
- Calculate Direct Sunlight Coefficients (CDS), using point-sky and high-resolution BSDF to get the direct sunlight contribution.
- Subtract the three-phase direct-sunlight-only results from the initial three-phase simulation and add the re-simulated accurate direct sunlight contribution.

Following the five-phase simulation, a subsequent glare analysis will begin. The glare analysis, conducted by `evalglare`, can be invoked to produce either the default results or the detailed. Choose detailed, if you would like to have additional information on glare source, size, etc. For calculating DGP the default output is sufficient.

The `evalglare` calculations are parallelized, so each assigned CPU is working on a different image simultaneously. The glare prediction follows the recommendations from Pierson et al. (2018), which states that for simulation work, with a view location close to the façade, the threshold method with 2000 cd/m^2 should be preferred. It should be mentioned that the workflow is developed for microstructures and its like. Macrostructures, like Venetian blinds, require a bit more work and tweaks by the user to account for the geometry of the shading in the *Direct Sunlight Coefficients*, CDS, calculation. The

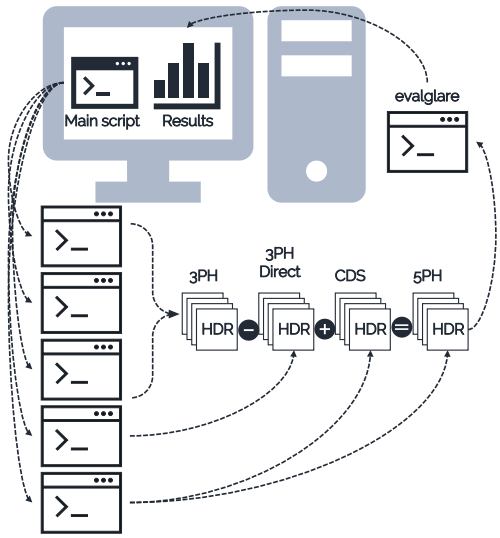

Figure 1: Conceptual overview of the simulation workflow.

workflow is used to compare glare predicted from simulations of the same scene, using varying BSDF resolution and rank of a microstructure. All the simulation work is done twice, using both regular BSDF and aBSDF (Ward (2018); Geisler-Moroder et al. (2021)). To investigate how BSDF properties bias the different aspects of discomfort glare, the *Vertical illuminance*, EV (Wienold (2010))(saturation glare), the *Modified Daylight Glare Index*, DGI$_{\mathrm{mod}}$ (Fisekis et al. (2003)) (contrast glare) and *Daylight Glare Probability*, DGP (Wienold and Christoffersen (2006)) (hybrid), are compared amongst each other for each simulation. Phase reuse is utilized for the first four steps, i.e., the initial three-phase simulation and the three-phase-direct-only. All the simulations are done in a relatively large space with three windows and a Window-Floor-Ratio of 30%, the room is furnished with simple furniture (tables and chairs). A wire-frame top view of the simulated space can be seen in Figure 2. All the simulations are conducted using annual climate data for Copenhagen with an hourly resolution. The surface reflectances used in the model can be seen in table 1. The findings regarding the biases on glare detection imposed by the BSDF properties are then used to determine the preferred BSDF rank and resolution, and simulation strategy (BSDF or aBSDF), which are crucial for a subsequent multi-orientation glare investigation of microstructures and alternative shading solutions.

Table 1: All materials are plastics, and have the same R,G and B reflectances. The specularity and roughness are zero for all materials used.

Surface	Reflectance
Walls	50%
Floor	20%
Ceiling	70%
Window frame	70%
Furniture	25%

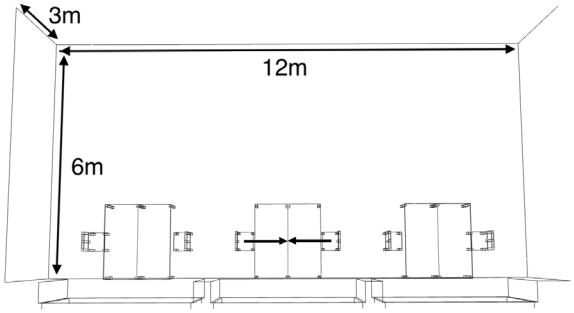

Figure 2: Wire-frame top-view of simulated space, arrows indicate the two view directions considered

Used fenestration systems

The microstructure used for the simulations is a MicroShade Film 60/14 (MS-F 60/14). The Microstructure is visualized in figure 3. The external Venetian blinds that are used in the comparison, are generated using the radiance native command `genblinds`. The blinds have a 45° tilt, are 10 cm wide, and are activated according to a shading schedule - based on a radiation study with a 200 W/m^2 threshold, which will provide the same thermal performance as the microstructure.

Results

Determining the BSDF best suited for predicting glare through microstructures

The first part of the results focuses on investigating the bias BSDF properties rank and resolution impose on the predicted glare, to determine the best suitable BSDF for microstructures. This investigation relies on simulations with a south facing façade and a viewing direction towards west. The simulation IDs in the plots refer to the used BSDF type and resolution and simulation strategy, e.g., ”45A” is a rank 4 tensor tree BSDF with resolution 4^5 = 1,024 and ”A” indicates that peak extraction has been used in the CDS calculation. An initial investigation considered both the *Mean-Absolute-Error* (MAE), *Mean-Bias-Error* (MBE), and *Root-Mean-Square-Error* (RMSE), however, as the different statistical measures did not yield much difference, only the MBE is included in this paper.

MAE; *Mean-Absolute-Error* - A measure of absolute error between paired observations.
MBE; *Mean-Bias-Error* - A measure of the biased error between paired observations.
RMSE; *Root-Mean-Square-Error* - A measure which penalizes larger errors more than smaller, due to the process of squaring the error.

Considering the saturation effects of glare expressed by the vertical illuminance, it is evident that the bias related to saturation glare is linked to the rank of the BSDF used, see Figure 4. The same plot also exhibits that the simulation strategy can have an impact on the observed bias, leaving only the resolution as a parameter that does not bias saturation glare. Considering only the contrast glare, expressed by CGI_{mod} in Figure 5, it can be seen the majority of the bias related to this type of glare is related to the resolution of the used BSDF. This bias, however, only affects simulations conducted using regular BSDFs in the CDS calculation. The same plot also exhibits that the rank of the BSDF does not impose any noteworthy bias on the predicted glare. Biases related to contrast glare are therefore primarily a concern if regular BSDFs are used. Though, it is a curiosity that low-resolution BSDFs seem to be more in accordance with the simulations conducted with peak extraction. When both effects are considered, as it is by DGP in Figure 6, it can be seen that all the previously encountered biases are somewhat present.

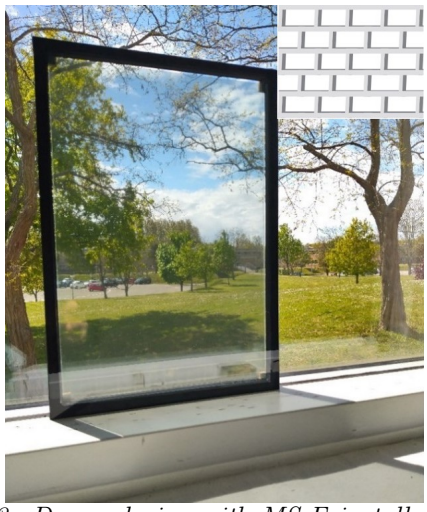

Figure 3: Demo glazing with MS-F installed put up against a common window without any film or microstructure installed. The shading effect of the microstructure can be seen by the shadow. Conceptual enlarged microstructure in top right corner.

The plot exhibit that the rank bias is still present, though highly limited. In terms of resolution, the plot suggests that the low-resolution BSDF (45) should be avoided. If aBSDFs are used instead, the plot shows that the resolution becomes obsolete. These plots thus imply that predicting glare through microstructures using a simulation-based approach, can be done with the five-phase method

Table 2: Percentage of occupation time (9-17) in discomfort glare categories according to DGP for the three types of fenestration systems investigated, windows on occupant right hand side

	DGP < 0.35			0.35 ≤ DGP < 0.40			0.40 ≤ DGP < 0.45			0.45 ≤ DGP		
Façade	**Low-E**	**Blinds**	**MS-F**	**Low-E**	**Blinds**	**MS-F**	**Low-E**	**Blinds**	**MS-F**	**Low-E**	**Blinds**	**MS-F**
S	0.54	0.63	0.86	0.07	0.09	0.01	0.06	0.09	0.01	0.32	0.19	0.12
SW	0.48	0.54	0.83	0.09	0.13	0.01	0.08	0.12	0.01	0.34	0.22	0.15
W	0.59	0.62	0.83	0.09	0.11	0.01	0.07	0.09	0.01	0.25	0.17	0.15
NW	0.75	0.76	0.93	0.11	0.12	0.01	0.04	0.04	0.00	0.10	0.08	0.06
N	0.94	0.94	1.00	0.06	0.06	0.00	0.00	0.00	0.00	0.00	0.00	0.00
NE	0.95	0.96	1.00	0.05	0.04	0.00	0.00	0.00	0.00	0.00	0.00	0.00
E	0.84	0.92	1.00	0.09	0.06	0.00	0.04	0.01	0.00	0.03	0.01	0.00
SE	0.71	0.81	0.95	0.08	0.08	0.00	0.07	0.05	0.00	0.14	0.06	0.04

NOTE View direction: ↻

Table 3: Percentage of occupation time (9-17) in discomfort glare categories according to DGP for the three types of fenestration systems investigated, windows on occupant left hand side

	DGP < 0.35			0.35 ≤ DGP < 0.40			0.40 ≤ DGP < 0.45			0.45 ≤ DGP		
Façade	**Low-E**	**Blinds**	**MS-F**	**Low-E**	**Blinds**	**MS-F**	**Low-E**	**Blinds**	**MS-F**	**Low-E**	**Blinds**	**MS-F**
S	0.48	0.58	0.83	0.07	0.10	0.01	0.09	0.10	0.01	0.36	0.21	0.14
SW	0.63	0.71	0.84	0.08	0.08	0.01	0.07	0.07	0.01	0.23	0.15	0.14
W	0.76	0.84	0.98	0.11	0.10	0.00	0.05	0.02	0.00	0.09	0.04	0.02
NW	0.91	0.94	1.00	0.08	0.05	0.00	0.01	0.00	0.00	0.00	0.00	0.00
N	0.95	0.95	1.00	0.05	0.05	0.00	0.00	0.00	0.00	0.00	0.00	0.00
NE	0.82	0.83	1.00	0.11	0.11	0.00	0.04	0.04	0.00	0.04	0.02	0.00
E	0.72	0.74	0.94	0.08	0.10	0.01	0.05	0.06	0.01	0.16	0.10	0.05
SE	0.51	0.53	0.83	0.08	0.12	0.01	0.07	0.11	0.01	0.35	0.23	0.14

NOTE View direction: ↺

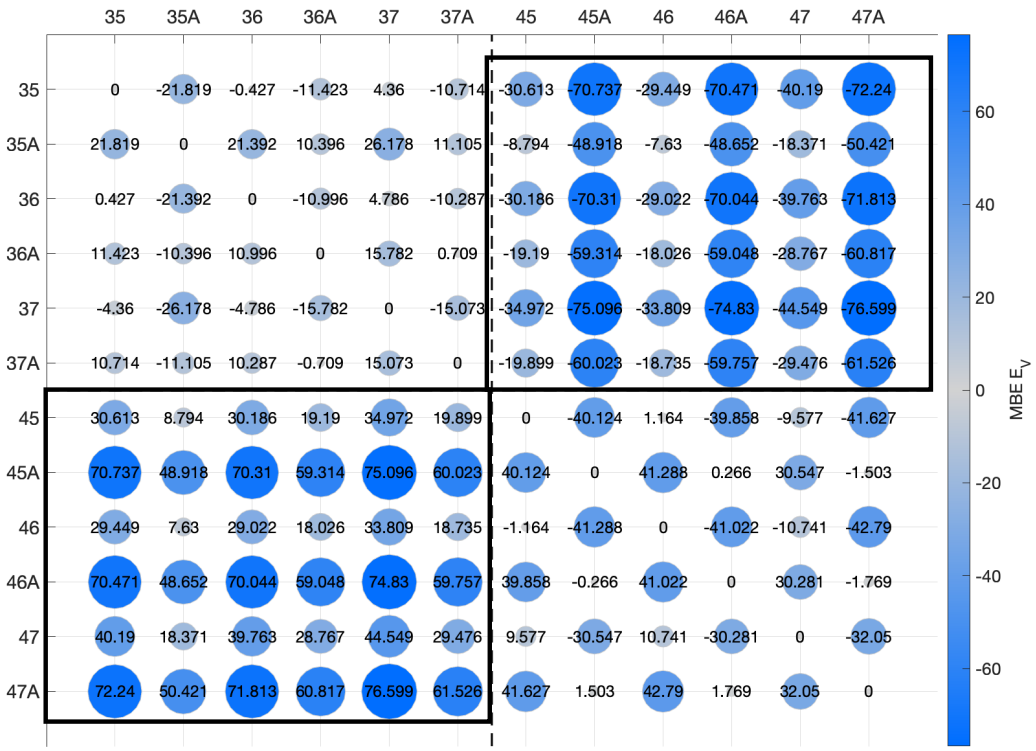

Figure 4: Mean-Biased-Error of Vertical Illuminance, EV, in lux (saturation glare). Bias marked in black boxes.

using a relative low-Resolution BSDF if peak extraction is used. The peak extraction algorithm can, however, not disregard the rank of the BSDF completely, which is especially evident if only saturation glare is considered. These results seem to be in correspondence with what was found in Apian-Bennewitz et al. (2021).

Glare evaluation - Microstructures performance as a glare protective mean

Based on the previous investigation, tensor tree 45 (simulated with peak extraction) has been identified as the most suited BSDF, in terms of accuracy and simulation time. The next part of the results will thus investigate the level of glare, expressed by DGP (in common office hours from 9-17 without DST), that one might expect from using a microstructure shading device. The glare predicted with a microstructure is compared to a Low-E window, without any additional shading device, and to a Low-E window with external Venetian blinds. Glare is evaluated for both view directions indicated in Figure 2 for the eight main orientations. The fact that the geometry does not change, allows for a high level of phase reuse. i.e., the daylight matrices are only calculated once as the room geometry stays unchanged, the view matrices are calculated once for each view direction and the CDS' is calculated once for each view direction and fenestration system. The only variable when all the initial matrices are produced is the sky matrices, which can be rotated at creation with `gendaymtx`, and the intermediate three-phase results, which are steps that do not require any additional ray-tracing, only matrix calculations. The results are exhibited as DGP "*flowers*", where each bar exhibits the percentage of occupied hours that falls into each of the discomfort glare categories. The view direction is stated according to the arrow in the center (always perpendicular to the façade orientation stated by the bar direction). The microstructure cannot, due to its transparent nature, be considered a glare protective mean. However by comparing the 16 façade orientation/view direction combinations for the microstructure to the Low-E window (see Figure 7a, 7b and 7c, 7d), it becomes evident that it has an impact on the expected amount of glare. Both of these fenestration systems will require additional glare protective means installed, though the difference between these two plots implies that the activation of the additional shading is much lower for the microstructure. Which ultimately will have an impact on how the occupants will perceive and rate the visual environment due to the lack of visual contact with the surroundings. An alternative to using a microstructure fenestration system could be to use external blinds, in terms of thermal performance. The simulations of the external blinds (activated according to the shading schedule) in Figure 7, exhibit that the blinds are not capable to provide a sufficient level of glare protection using the current shading schedule.

Comparing the performance of the external blinds to the microstructure (Figure 7e 7f and 7a 7b) exhibits that the microstructure performs better than the blinds with the current control algorithm. Some of the difference between these two fenestration systems could be ascribed to the fact that the microstructure also has vertical elements, which will provide additional shading when the sun gets more into the field-of-view of the occupant. Some of it could also be ascribed to the current control algorithm and the fact that only two states of the blind are consid-

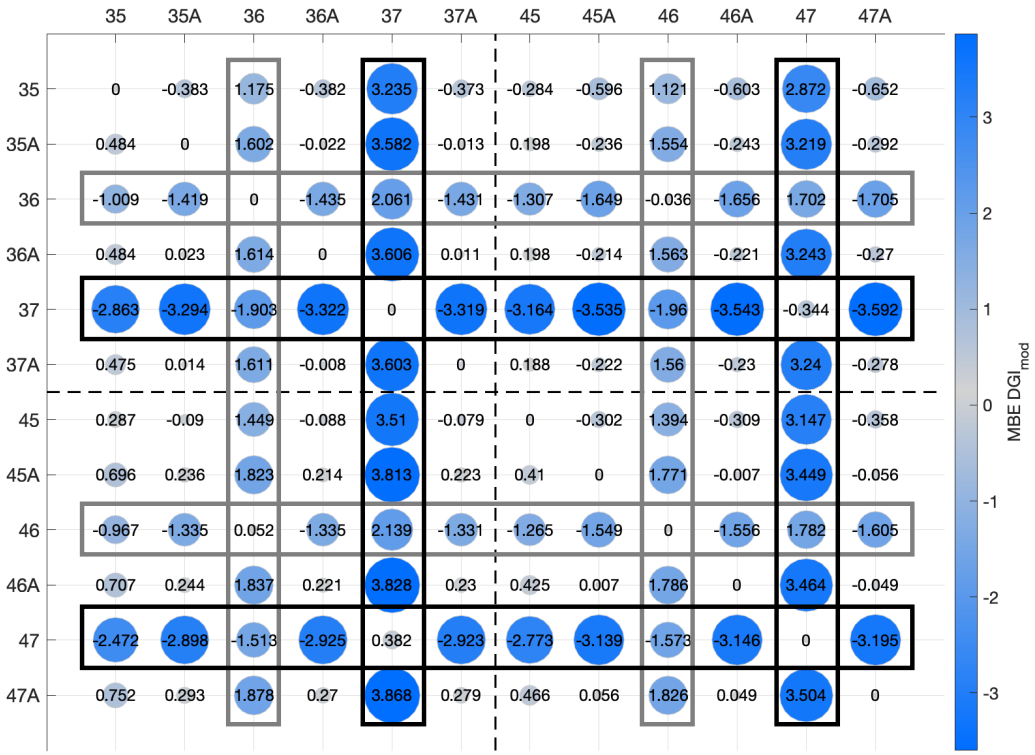

Figure 5: Mean-Biased-Error of Modified Daylight Glare Index, DGI_{mod} (contrast glare). Bias marked with black and grey boxes.

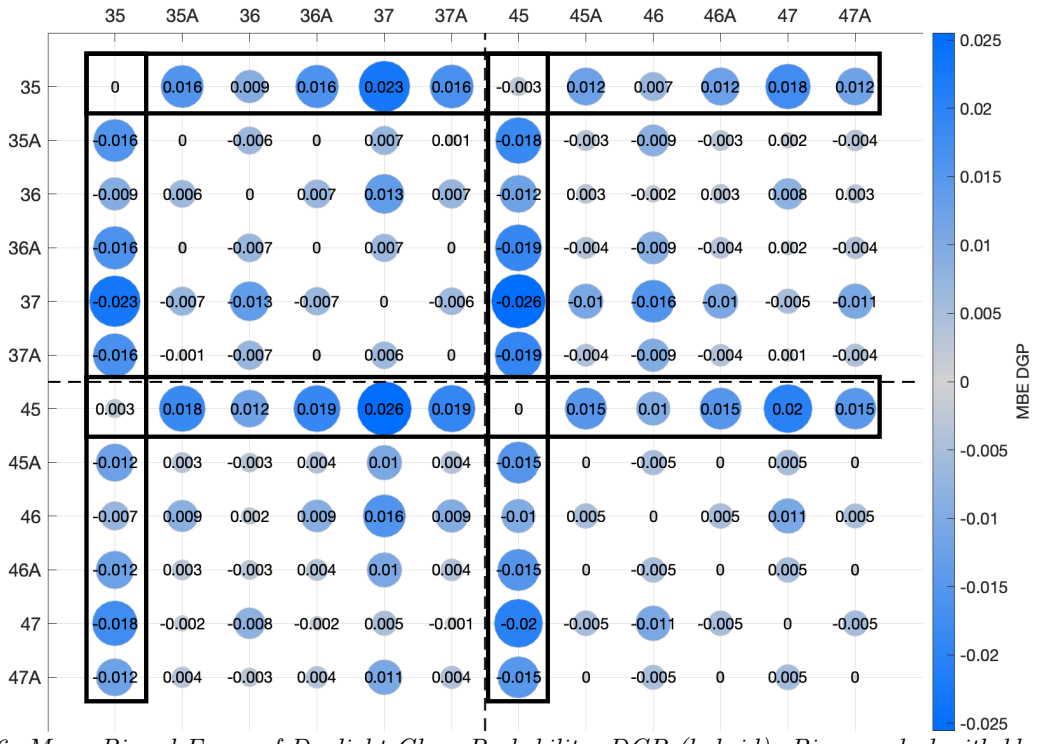

Figure 6: Mean-Biased-Error of Daylight Glare Probability, DGP (hybrid). Bias marked with black lines.

ered in this study. Considering the situation where the façade is facing south, the activation time of the blinds (between 9-17) is 52%, this number depends on the control strategy (in this case the 200W/m^2 threshold), though by introducing more states of the blind the glare protective ability should increase, lowering the percentage of occupied hours falling into the worst rated category of discomfort glare. In addition to the control algorithm, a real-life application of this type of shading would likely have a manual overwrite. Comparing the percentage of occupied hours in the different categories, in Table 2 and 3, shows that the microstructure will provide an equal or better level of glare protection for all the considered orientations, compared to the blinds. The difference is peaking in Table 2 at façade orientation S and SW with a 7% difference at in Table 3 at façade orientation SE with a 9% difference. The same tables also substantiate the figures 7b and 7a, showing that the microstructure will not provide a graduating level of glare protection only yielding a small percentage of occupied hours falling into the two middle categories of discomfort glare.

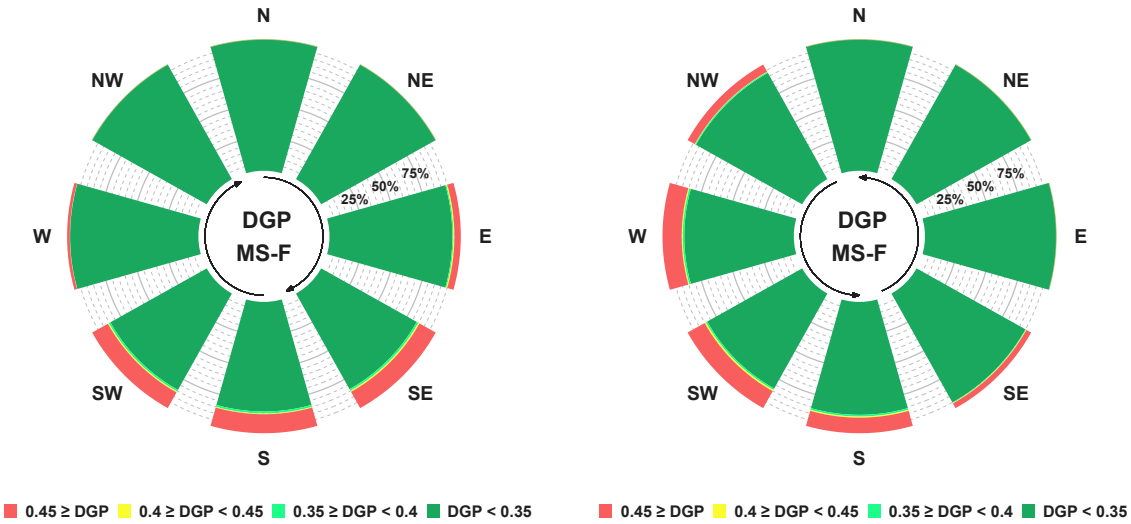

(a) DGP Flower MS-F window, View ↻ *(b) DGP Flower MS-F window, View ↻*

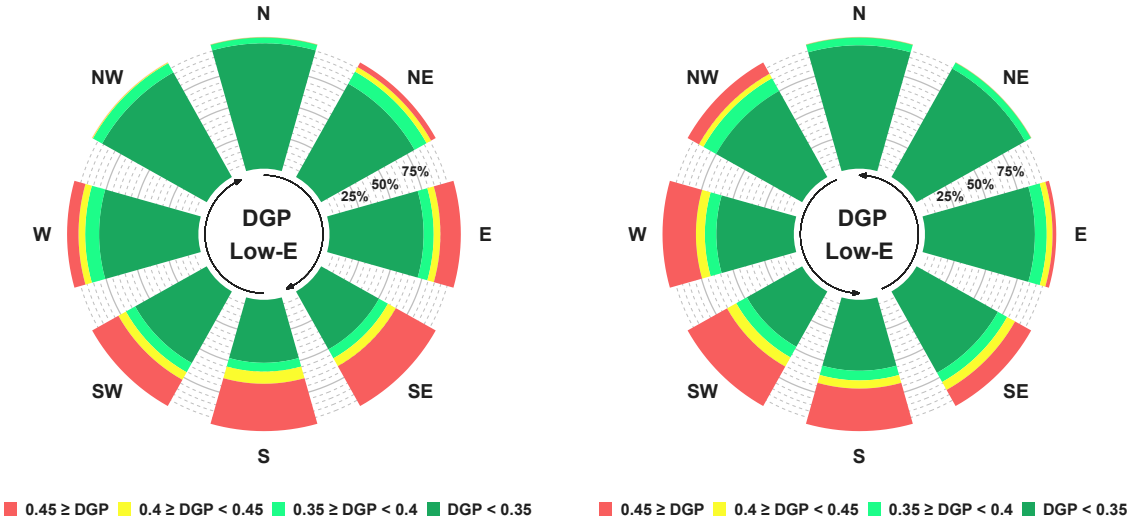

(c) DGP Flower Low-E window, View ↻ *(d) DGP Flower Low-E window, View ↻*

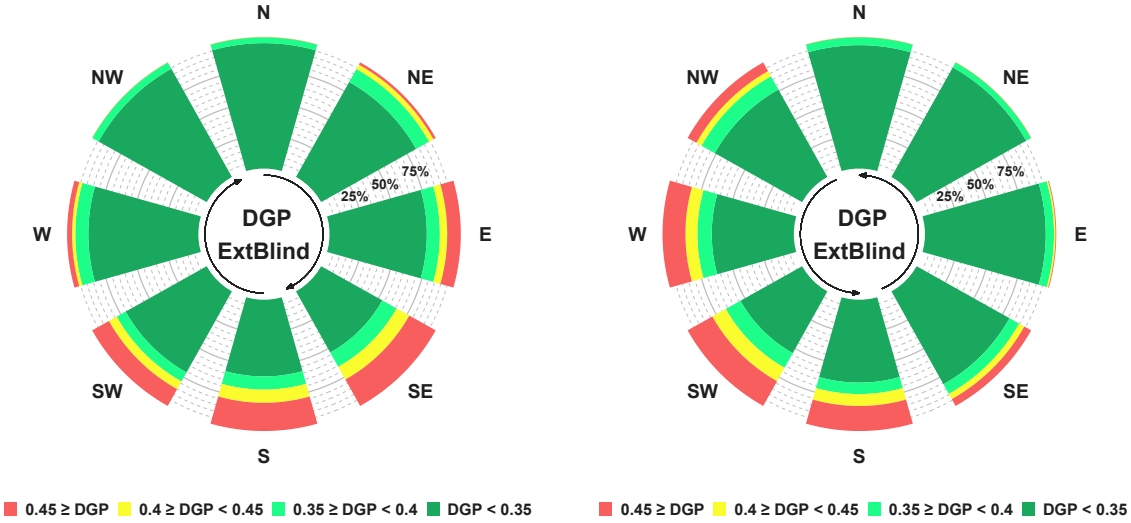

(e) DGP Flower Low-E window + Blinds, View ↻ *(f) DGP Flower Low-E window + Blinds, View ↻*

Figure 7: DGP flowers for various fenestration systems, exhibiting the percentage of occupied hours (9-17) which are falling into the different categories of discomfort glare. The black arrow in the center states the view direction, always perpendicular to façade orientation.

Discussion

The results regarding the Low-E window follow expectations, being the worst type of fenestration system, in terms of glare protection. In a real-life application, it is however likely that this window would be combined with some sort of internal shading, controlled by the occupants. In this study this situation mainly serves as a benchmark, exhibiting what to expect if no considerations regarding glare are made. The results from these simulations thus also show, that glare will be an issue for most façade orientations where the sun at some point will be in the field-of-view. Both the microstructure and the external blinds are mainly considered a solution used for accommodating overheating issues. The results exhibit, in terms of the blinds, that even though the blinds would have the ability to remediate some of these glare issues with the current strategy, it is not sufficient. A more elaborate control strategy should therefore be considered, using more shading states and most likely also a lower activation threshold. Alternatively, the system should have a manual overwrite, leaving the occupants responsible for their visual environment. Though this may interfere with the control strategy which mainly considers the thermal environment. The microstructure provides sufficient glare protection for four (almost five) of the eight considered orientations. However, this shading is static, so additional internal shading will have to be installed. The activation time of this shading will be around 10% of occupied hours (allowing 5% of occupied hours in the worst category) and will have to be controlled by the occupants without interfering with any thermal control strategy. The same solution could also be considered for the external blinds, though the activation time will be increased by up to 17% of occupied hours (still allowing 5% of occupied hours in the worst category). If a higher level of glare protection is desired, i.e. no more than 5% of occupied hours exceed a DGP of 0.40, the activation time for the blinds will increase even further for some orientations. This is not the case for the additional shading that should be used in combination with the microstructure.

Conclusion

The preliminary investigation of how various BSDF parameters bias the predicted glare has shown that BSDF rank is related to saturation-based glare and BSDF resolution to contrast. The investigation has, however, also shown that the recently introduced peak extraction algorithm, aBSDF, will resolve much of the resolution-related bias, making it possible to use lower resolution BSDFs in combination with peak extraction for systems with a high level of specular transmission like curtains and microstructures, all in agreement with what is found in Apian-Bennewitz et al. (2021).

Based on the simulations and glare predictions conducted in this study, can it be concluded that none of the investigated fenestration systems, with the current control algorithm, can be considered sufficient glare protection for no more than half of the considered orientations. The microstructure is found to perform best under the current conditions, yielding the lowest percentage of occupied hours in the worst categories. The microstructure will however require an additional type of internal solar shading installed to be able to cope with excessive glare. For the external blinds, it is possible to accommodate some of the glare conditions with a more elaborate control strategy and/or manual overwrite. Though, this will, everything equal, have a greater impact on the visual contact with the surroundings and potentially also the thermal environment, as it will require the blinds to close further down and be activated more often. Based on these findings, it can therefore be concluded to be more beneficial in terms of glare (and the visual environment, if activation time of additional shading is considered) to use a microstructure, if the control strategy of the blinds is not elaborate enough. Even though the overall performance of the microstructure does not make it a glare-protective solar shading.

References

Apian-Bennewitz, P., J. de Boer, B. Bueno, B. Deroisy, Y. Fang, D. Geisler-Moroder, L. O. Grobe, J. C. Jonsson, E. S. Lee, Z. Tian, T. Wang, G. J. Ward, H. R. Wilson, and Y. Wu (2021, 10). Analysis and evaluation of bsdf characterization of daylighting systems.

Fisekis, K., M. Davies, M. Kolokotroni, and P. Langford (2003). Prediction of discomfort glare from windows. *Lighting Research & Technology 35*(4), 360–369.

IEA Solar Heating and Cooling Programme (2021, 1). *BSDF Generation Procedures for Daylighting Systems*.

Geisler-Moroder, D., E. S. Lee, and G. J. Ward (2017, 08/2018). Validation of the five-phase method for simulating complex fenestration systems with radiance against field measurements.

McNeil, A. (2013). The Five-Phase Method for Simulating Complex Fenestration with Radiance.

McNeil, A. (2015). genBSDF tutorial.

Pierson, C., J. Wienold, and M. Bodart (2018). Daylight discomfort glare evaluation with evalglare: Influence of parameters and methods on the accuracy of discomfort glare prediction. *Buildings 8*(8), 94.

Subramaniam, S. (2017). Daylighting simulations with radiance using matrix-based methods.

Ward, G. (2018). Radiance updates, 17th international radiance workshop, loughborough, uk.

Wienold, J. (2010). Dynamic daylight glare evaluation.

Wienold, J. and J. Christoffersen (2006). Evaluation methods and development of a new glare prediction model for daylight environments with the use of CCD cameras. *Energy and Buildings 38*(7), 743–757.